International Journal of Architectural, Civil and Construction Sciences
ISSN: 2415-1734
Vol:3, No:5, 2009

Investigation into the Bond between CFRP and Steel Plates

S. Fawzia, and M. A. Karim

***Abstract*—**The use of externally bonded Carbon Fiber Reinforced Polymer (CFRP) reinforcement has proven to be an effective technique to strengthen steel structures. An experimental study on CFRP bonded steel plate with double strap joint has been conducted and specimens are tested under tensile loadings. An empirical model has been developed using stress-based approach to predict ultimate capacity of the CFRP bonded steel structure. The results from the model are comparable with the experimental result with a reasonable accuracy.

***Keywords*—**Carbon fibre reinforced polymer, shear stress, slip, effective bond, steel structure.

I. Introduction

A large number of steel structures and bridges are deemed structurally deficient. This is either because the infrastructure continues to age and deteriorate or the strength or deformation capacity of the existing older infrastructure does not meet the current code requirements, e.g., in high seismic regions. Thus, the need for more efficient retrofit methods has increased in recent years. Currently, carbon fiber reinforced polymer (CFRP) composite is popular for strengthening or retrofitting steel structures. The critical issue for strengthening steel structure is the bond, and therefore the properties of the bonding materials are very important. In this study tests have been done to measure the actual properties of the materials used in the experiment. An experimental investigation has been conducted for CFRP bonded steel plate under static load condition to predict the bonding strength.

II. Properties of Bonding Materials

Concrete, steel and timber have been the prominent materials utilized in the construction industry for many decades and this situation is likely to continue to be the case for the next decade or so. However advanced materials and in particular the advanced polymer composites have been combined with the more conventional materials for over a decade and the combination have produced a new generation in structural system. Composite materials like FRP fibre reinforced composites, GFRP glass fibre reinforced polymer, CFRP carbon fibre reinforced polymer and Aramid composites, have been used for strengthening RC structures in both practical application and research. Typical stress strain curves for CFRP, GFRP, concrete and steel show the brittle behaviour of FRP composites and concrete and the ductile behaviour of steel. This has two major structural consequences. First, these materials do not possess the ductility of steel, and second, owing to this lack of ductility, the redistribution of stresses in FRP composite is restricted. Consequently, the methods used to strengthen steel structures with CFRP composite cannot be the same as existing methods for strengthening RC structures [1].

Fig. 1 Test set up of CFRP

There are many resins for strengthening concrete structures with CFRP at present in the world, and the key mechanical properties of adhesives for strengthening structures are the strength, elastic modulus, elongation percentage. Significant difference exists between steel and concrete in many aspects such as mechanical property, physical property and surface state, therefore some special requirements need for the adhesive selection. Adhesive is to be stronger to get better performance while considering steel structure strengthening. There has always been a gap between manufacturer claimed properties and actual properties of the materials. Manufacturers will often supply indicative property data for adhesive bonds. In order to obtain an accurate value for material properties, testing must have been conducted on similar material [2]. Different types of CFRP and adhesives are studied and the best one has been selected based on manufacturer provided data. However, a series of tensile coupon tests were conducted to determine the actual

Sabrina Fawzia is with School of Urban Development, Faculty of Built Environment & Engineering, Queensland University of Technology, Australia (phone: 617-31381012; fax: 617-31381170; e-mail: sabrina.fawzia@qut.edu.au).
Azharul Karim is with School of Engineering System, Faculty of Built Environment & Engineering, Queensland University of Technology, Australia (phone: 617-31386879; fax: 617-31381516; e-mail: azharul.karim@qut.edu.au).

properties of the materials and evaluate manufacturer provided data. Test set up for CFRP and adhesive are shown in Fig. 1 and 2 respectively. Test results of CFRP and adhesive has been listed in Table I and II respectively.

TABLE I
PROPERTIES OF CFRP

Specimen label	Tensile strength MPa	Ultimate strain	Elastic Modulus GPa
NF1	2393	0.008	284
NF2	3153	0.015	205
NF3	2478	0.012	201
Mean	2675	0.012	230
COV	0.156	0.295	0.203

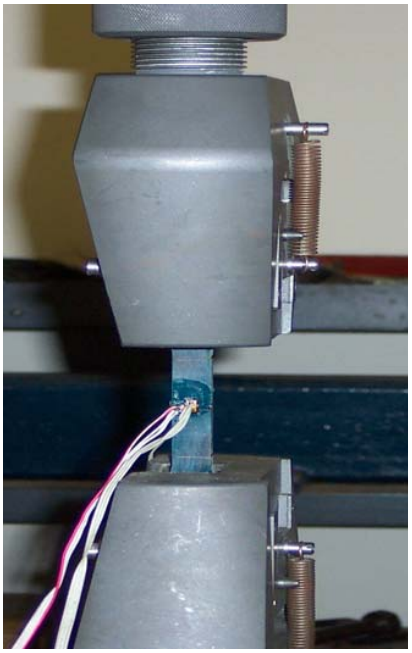

Fig. 2 Test set up of adhesive

TABLE II
PROPERTIES OF ADHESIVE

Specimen label	Tensile strength MPa	Ultimate strain	Elastic modulus MPa	Poisson's ratio
AR1	29.9	0.020	1940	0.35
AR2	30.1	0.020	2095	0.40
AR3	28.6	0.027	1787	0.34
AR4	27.5	0.022	1916	0.38
AR5	27.0	0.029	1767	0.34
Mean	28.6	0.024	1901	0.36
COV	0.048	0.164	0.070	0.081

Specimen NF2 (Table I) shows higher tensile strength than others, which indicates that quality of specimens preparation is very important. NF2 achieved the highest ultimate strain of 1.5% among all specimens. The mean value of tensile strength is 2675 MPa with a COV of 0.156. The measured elastic modulus is 230 GPa and ultimate strain is 1.2%, while the manufacturer specified values are 240 GPa and 1.55% respectively. Table II shows the average tensile strength of adhesive is 28.6 MPa, indicating that there is a little difference with the manufacturer-provided tensile strength of 32 MPa. The measured ultimate strain of 2.4% is lower than the manufacturer's value of 4%, but the modulus is the same as the manufacturer's value of 1900MPa.

III. TEST SPECIMENS FOR BOND STRENGTH OF STEEL-CFRP JOINTS

The steel plates were grinded by angle grinder in the area to be bonded to ensure better mechanical interlocking. The surfaces were cleaned with acetone to remove grease, oil and rust. Two steel plates were kept perfectly horizontal in position in a jig before applying adhesives and CFRP. The horizontal position was maintained by a level device. The CFRP was cut to the prescribed dimensions and adhesives were mixed according to the manufacturer's specifications.

A small amount of adhesive was applied first at the cross-sectional surfaces of the steel plate. Two plates were bonded together. The jointed plate was cured for 24 hours. Then adhesive was applied along the bond length of the steel plate which was grinded and cleaned with acetone immediately before the bonding process was carried out. Then the first layer of CFRP sheet was placed on top of the adhesive. The sample was ribbed rolled to squeeze out excess adhesives. Following the above procedures, another two layers of CFRP sheets were applied on top of the first layer and the specimen was cured for a few days. After that, three layers of CFRP were applied on the other side of the steel plate following the same procedure. The specimens were then cured for 7 days at ambient temperature and post cured for one day at 70^{o}C. Fig. 3 shows the bare steel plate (top), the grinded steel plate (middle) and finally the CFRP bonded to the steel plate (bottom).

Fig. 3 Bare steel plate, grinded steel plate and bonded CFRP

A schematic view of a specimen is shown in Fig. 4 which indicates that the length l_1 was always kept less than l_2 to ensure that the failure occurred on one end only. Several foil strain gauges (Fig. 5) were attached to the CFRP bonded length; one at the joint and others in every 15 mm along the bonded length. A string pot was attached to the specimen to

obtain the total displacement of the specimen. The LVDT (linear variable displacement transducer) was fixed to obtain the slip between the CFRP sheet and the steel plate. Test specimen loaded to tension in a Baldwin Universal Testing machine until failure. A data acquisition system was used to record the data from the strain gauge as well as from the machine. A digital video recorder and a high-speed video recorder were used to capture the crack propagation. The high-speed video recorder recorded at 500 frames per second.

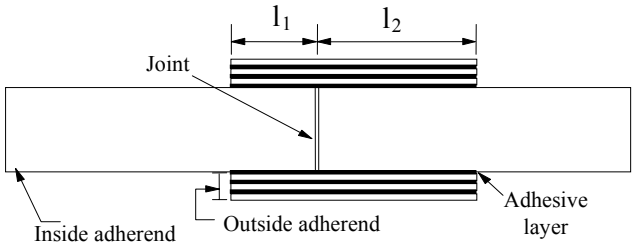

Fig. 4 Schematic view of the specimen (not to scale)

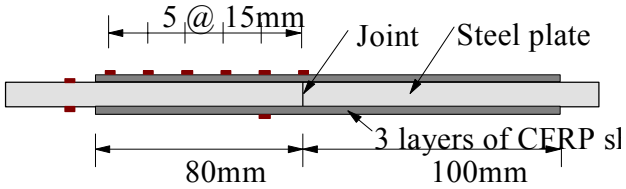

Fig. 5 Location of strain gauges of a typical specimen (not to scale)

IV. Test Results

Results from the test are presented in Table III. In the first column N stands for normal modulus CFRP sheet, A stands for adhesive and the number represent the bond lengths. The specimens failed by combined failure, which is a combination of steel adhesive interface debonding and CFRP delamination. More details about this failure mode can be found in Zhao and Zhang [3]. Specimens failed by debonding of the CFRP sheet due to high shear stresses in the steel-adhesive interface. Debonding was initiated at the loaded end near the joint and propagated towards the end of the CFRP sheet. The failure mode of normal modulus CFRP sheet with adhesive joint for steel strengthening actually depends upon the adhesive properties rather than the CFRP properties.

TABLE III
Test Results

Specimen level	Bond length mm	Ultimate Load kN
NA20	20	33.7
NA40	40	49.9
NA50	50	69.8
NA60	60	58.8
NA70	70	80.8
NA80	80	81.3
NA90	90	69.8
NA150	150	91
NA200	200	92.6
NA250	250	97.2

V. Strain along the Bonded Length

The data obtained from the strain gauges on the top layer of CFRP were used to create plots of strain versus distance from the steel joint. The top strain was different from the average composite strain as the strain could vary across the layers of the composite. This variation was measured experimentally for circular tube strengthened by CFRP sheet and for steel plate [4]. In this study it was assumed that the measured strain represented the average CFRP strain. The distributions of strain along the bond length for different load levels are plotted in Figs. 6-9 for each bond length of the specimens.

The distance shown in the figures is measured from the joint location because the steel joint is considered as the loaded edge of the specimen. At low load levels, the distributions show a gradual decline from the peak near the steel joint to the other end. As the load increases, strain values also increase. At low load levels, the distributions have the largest slope near the steel joint. As the load increases, the maximum slope shifts away from the joint. This means that at low load levels the distribution is highly nonlinear, and gradually approaches an almost linear shape as the load increases. Thus it can be concluded that as the load increases, redistribution of the bond stress along the bond length occurs as a result of changes in the state of the bond.

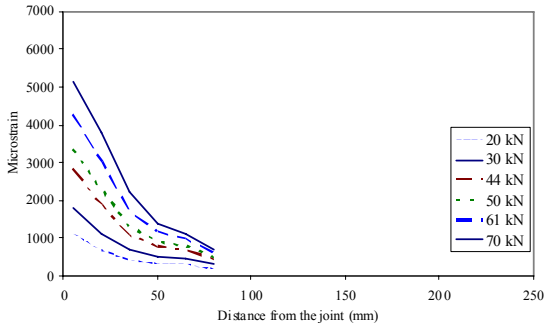

Fig. 6 Distribution of strain along the bond length 80mm of the specimen

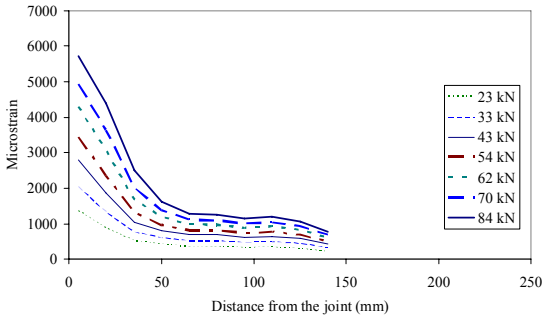

Fig. 7 Distribution of strain along the bond length 150 mm of the specimen

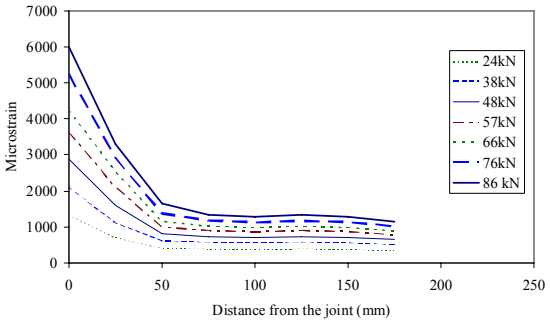

Fig. 8 Distribution of strain along the bond length 200mm of the specimen

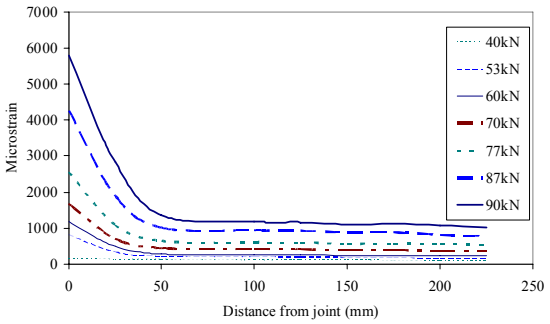

Fig. 9 Distribution of strain along the bond length

VI. Relationship of Shear Stress and Slip along the Bonded Length

In the present study, the average experimental shear stress was calculated from the readings of strain gauges mounted on the top surface of the CFRP sheet [5]. The calculated shear stress distributions along the distance away from the "steel joint" are shown in Fig. 10 at different load ratios. Load ratio can be defined as the corresponding load divided by the maximum ultimate load achieved in the test.

It can be seen in figure that initially, shear stress is highest at the loaded end. When the peak shear stress starts decreasing at the loaded edge and moves away from the joint, the linear stage of the load-displacement curve ends, and the softening stage starts. When the shear stress at the loaded end reduces to zero, the ultimate load of the specimen is reached. These stages of development are the same as those described for FRP-to-concrete bonded joints [5]. The theoretical stress distribution for bond between CFRP and concrete can be found in Yuan et al.[5]. The theory states that shear stress is zero at the loaded edge when it reaches peak load, indicating occurrence of debonding.

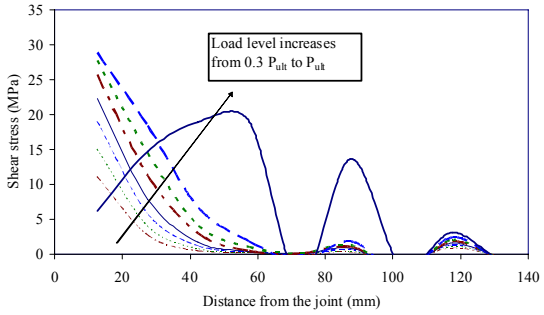

Fig. 10 Shear stress distribution of bond length 200mm of the specimen

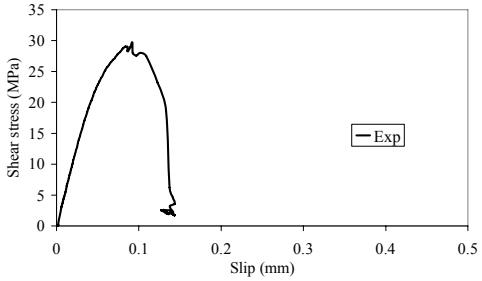

Fig. 11 Shear stress and slip relationships of experimental results

Local slips were calculated by integrating measured strain distribution along the bond length. This local slip is the relative displacement between the CFRP sheet and the steel plate. Calculated shear stresses and slips are combined to obtain the local shear stress-slip curves. The local shear stress slip relationship is reasonably consistent between different locations on the same specimen [6]. Therefore Fig. 11 presented here shows maximum shear stress slip relationships from different locations on the same specimen. According to Fig. 11, the results for maximum shear stress, slip at maximum shear stress (initial slip) and maximum slip of the specimen are 28MPa, 0.07mm and 0.14mm respectively.

Existing work on shear stress-slip relationships for CFRP-strengthened steel structures is limited. Recently, the bond-slip relationship relating the interfacial shear stress to the interfacial slip has been investigated for CFRP-plate-strengthened steel structures by Xia and Teng [6], who presented a bilinear relationship between shear stress and slip. Fig. 11 also shows a bilinear shape of the curve.

The expression for shear stress can be derived from regression analyses as:

$$\tau = 414.17s + 1 \quad \text{[Elastic region]} \qquad (1)$$

The initial stage is the elastic region which is linear ascending prior to softening.

$$\tau = -587.63s + 83.7 \quad \text{[Softening region]} \qquad (2)$$

Eq.(1) is representing elastic stage and Eq. (2) is representing softening stage of load deflection curve. The elastic stage is followed by initiation of softening, then propagation of the softening zone. At the end of the softening zone, debonding starts.

VII. Imperial Model for Bond Strength by Using Stress Based Approach

The load carrying capacity for any bond length can be expressed as Eq. (3) and Eq. (4) [7], assuming that the load is linearly proportional to the bond length:

$$P_{CFRP} = l_1 . \frac{P_{ult}}{l_{eff}} \qquad (3)$$

if $l_1 < l_{eff}$

$$P_{CFRP} = P_{ult} \qquad (4)$$

if $l_1 > l_{eff}$

where l_{eff} is effective bond length 75mm [7]
P_{CFRP} Ultimate capacity of bond length l_1
P_{ult} Ultimate capacity of bond length l_{eff}

The imperial model can be developed by using stress based approach is expressed in Eq. (5):

$$P_{ult} = .8\tau w l_{eff} \qquad (5)$$

Where, τ = Shear stress 28 Mpa [Fig. 11]
w = Width of the bonding area

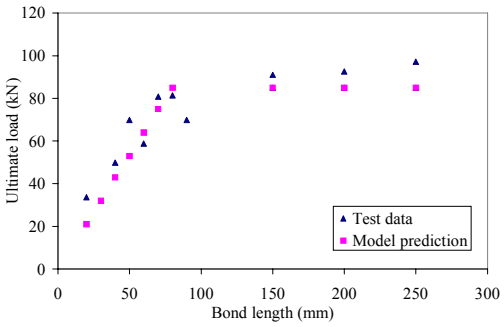

Fig. 12 Comparison of experimental and imperial model result

The maximum shear stress from the experiment has been used to predict the ultimate load carrying capacity. Fig. 12 shows reasonably good agreement of the model prediction with the tested result. If bonding length varies between 20 to 80 the forces in CFRP varies as long as $l_1 < l_{eff}$. The load carrying capacity of any bond length which exceeds the effective bond length is equal to ultimate load carrying capacity of effective bond length.

VIII. Conclusion

The strain distribution at low load levels is highly nonlinear, and gradually approaches an almost linear shape as the load increases. The shear stress and slip relationship is a bilinear relationship. A proposed empirical load-carrying capacity model based on stress-based approach for steel plate strengthened by normal modulus CFRP is found to be in good agreement with the test results.

Appendix

The authors acknowledge the contribution of Civil engineering laboratory staff at Monash university for the setup of the test equipment. MBT, Vantico & OneSteel Market Mills, Australia Pte Ltd provided Fiber, Epoxy and steel tubes, respectively.

References

[1] Fawzia, S., Al-Mahaidi, R., Zhao, X.L. and Rizkalla, S., "Comparative Study of Failure Mechanisms in Steel and Concrete Members Strengthened with CFRP Composites", Developments in Mechanics of Structures and Materials, Deeks, A.J. and Hao, H. (eds), Balkema Publishers, pp.71-76 London, 2004.
[2] Moy, S.S.J., "FRP composites: life extension and strengthening of metallic structures", ICE Design and Practice Guides, Thomas Telford, London, 2001, UK.
[3] Zhao, X.L. and Zhang, L., "State-of-the-art review on FRP strengthened steel structures", Engineering Structures, Vol 29(8), pp.1808-1823, 2007.
[4] Fawzia, S., Al-Mahaidi, R., Zhao, X.L. and Rizkalla, S., "Strengthening of circular hollow steel tubular sections using high modulus CFRP sheets", Construction and Building Materials, Vol 21(4), pp.839-845, 2007.
[5] Yuan, H., Teng, J.G., Seracino, R., Wu, Z.S. and Yao, J., "Full-range behaviour of FRP-to-concrete bonded joints", Engineering Structures, Vol 26(5), pp.553-565, 2004.
[6] Xia, S. H. and Teng, J. G., "Behaviour of FRP-to-steel bonded joints." Proceedings of the International Symposium on Bond Behaviour of FRP in Structures (BBFS 2005), pp.419-426, Hong Kong, 2005.
[7] Fawzia, S., "Bond Characteristics between Steel and Carbon Fibre Reinforced Polymer (CFRP) Composites", Ph.D thesis, Monash University, Australia 2007.